Effect of the CuAl$_2$O$_4$ and CuAlO$_2$ Phases in Catalytic Wet Air Oxidation of ETBE and TAME using CuO/γ-Al$_2$O$_3$ catalysts

Cecilia Sánchez-Trinidad,[a] Gloria del Angel,[b] Gilberto Torres-Torres,*[a] Adrián Cervantes-Uribe,[a] A. Abiu Silahua Pavón,[a] Zenaida Guerra-Que,[a, c] Juan Carlos Arévalo-Pérez,[a] and Francisco J. Tzompantzi-Morales[b]

This paper studies Cu/Al$_2$O$_3$ catalysts, synthesized in two ways: copper deposit in the synthesis of alumina (sol gel) and incipient impregnation stabilized at 400 °C. The materials were characterized by X-ray diffraction studies, nitrogen physisorption, temperature programmed reduction of H$_2$, dehydration of isopropanol, scanning electronic microscopy, transmission electronic microscopy, which were evaluated in the liquid phase oxidation reaction of ethyl tert-butyl ether and tert-amyl methyl ether. The formation of CuAl$_2$O$_4$ and CuAlO$_2$ in the samples synthesized by sol gel, led to a modification of the texture, thus resulting in an expansion of the specific area of the materials. CuAl$_2$O$_4$ and CuAlO$_2$ have been identified by DRX from a content of 10% Copper, the first showed the highest intensity with this technique. In the same way, these species favor the presence of Lewis acid sites; this is reflected in the materials with (Di-isopropyl Ether) DIPE of 96.7% and 91.1% for the samples SAlCu5 and SAlCu15 respectively. The catalytic activity of the materials prepared by sol gel is in the function of the number of surface acid sites, the smaller particle size of the Cu and the surface of the contact, in the case of the ETBE meanwhile for TAME the activity was based mainly on the strength of the present acid sites. With impregnated materials, the activity is attributed to the smaller particle size of the Cu and the greater strength of the surface acid sites in the solid. The formation of spinel species inhibits the leaching phenomenon in the reaction milieu.

1. Introduction

The species that compose a catalyst, as well as the interactions between them, significantly affect certain chemical reactions .[1] For a long time, the interactions between metal and its support have been studied in heterogeneous catalysis since 1970, when the concept of "metal-support strong interaction" was introduced for the first time.[2] To understand this phenomenon, model reactions have been used to determine and indicate the

[a] C. Sánchez-Trinidad, G. Torres-Torres, A. Cervantes-Uribe, A. A. S. Pavón, Z. Guerra-Que, J. C. Arévalo-Pérez
Universidad Juárez Autónoma de Tabasco, Laboratorio de Nanomateriales Catalíticos Aplicados al Desarrollo de Fuentes de Energía y Remediación Ambiental, Centro de Investigación de Ciencia y Tecnología Aplicada de Tabasco (CICTAT), DACB, Km. 1 carretera Cunduacán-Jalpa de Méndez AP. 24, C.P. 86690, Cunduacán Tabasco, México
Fax: +52 19143360928
Tel: +52 19143360300
E-mail: gilberto.torres@ujat.mx
torremensajes@gmail.com
[b] G. del Angel, F. J. Tzompantzi-Morales
Universidad Autónoma Metropolitana-Unidad Iztapalapa, Departamento de Química, Área de Catálisis, Av. San Rafael Atlixco 186, C.P. 09340; A. P. 55–534 México D.F., México
[c] Z. Guerra-Que
Instituto Tecnológico de Villahermosa, Departamento de Ing. Química-Bioquímica-Ambiental, Km. 3.5 Carretera Villahermosa-Frontera, Cd. Industrial, C.P. 86010 Villahermosa, Tabasco, México

interaction of the elements that constitute a catalyst, this is the case of the workgroup Wachs[3] and Reddy,[4] to name a few. The interaction between metal-oxide of metal or between metal oxides exhibit a variation due to the structural complexity resulting in the formation of interacting species, this is the case of the copper-alumina binomial.[5] So, metal-support interactions have been studied during the synthesis of copper catalysts, mainly because they are generally strong, which limits the load of the metal that is deposited to avoid large agglomerates that promote sintering and nucleation.[6] Strong copper-support interactions can cause the formation of new crystalline phases during catalyst preparation. Although the formation of a new phase with copper implies a loss of the active phase, in some cases it may represent a benefit. For example, the formation of a solid Cu–Al$_2$O$_3$ solution or aluminates. The used synthesis methods are usually conventional impregnation processes, causing a heterogeneous distribution of the species on the surface and, in some cases, the reduction of the surface area,[7] which is why it is very important to use new methodologies that allow obtaining catalysts with high dispersion of the constituent metals, modified with promoter species, and that are characterized by having a good activity, selectivity and interaction between the species at relatively low temperatures. The copper aluminate nanocomposites spinel type (CuAl$_2$O$_4$, CuAlO$_2$) are of interest due to their low cost, thermal stability, non-toxic, high mechanical resistance, hydrophobicity and low surface acidity,[8] characteristics that make them attractive in various fields, for example, photocatalysts for the degradation of organic pollutants,
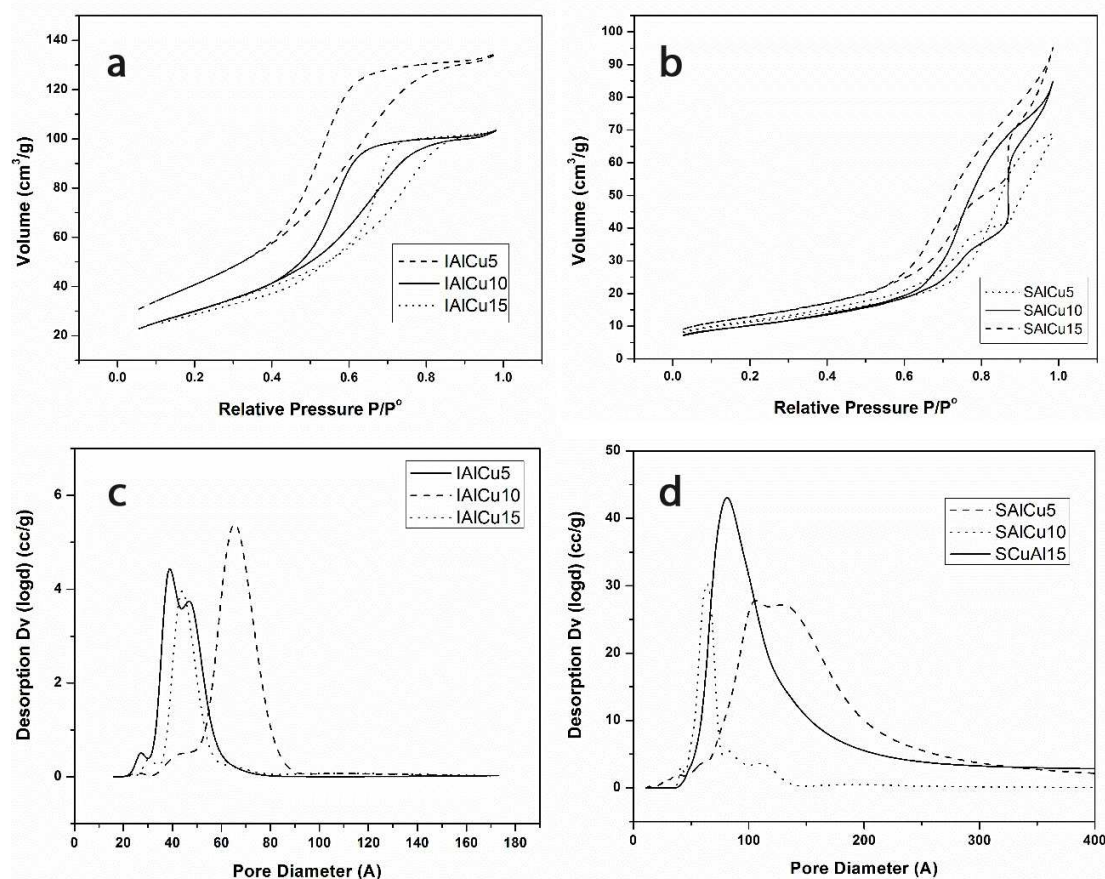
Figure 1. Adsorption-desorption isotherms a) Method of impregnation b) Method sol gel, pore distribution for the catalysts synthesized c) Impregnation d) Sol gel.

magnetic materials, rechargeable batteries, medicine, recycling of nuclear fuel and oxidation of organic molecules.[9–11]

Catalytic wet air oxidation (CWAO) of contaminants has become a promising technique for solving a wide variety of water pollution problems.[12] Several studies have been carried out to develop suitable catalysts to be applied to this technique in the last decades. The catalysts supported by noble metals have proved to be the most important to oxidize a wide variety of contaminants by CWAO[13–17] Oxidation in the liquid phase is a treatment capable of completely oxidizing these compounds, in besides maximizing selectivity in CO_2.[18] However, copper catalysts, usually industrial CuO/Al_2O_3 with 10% loading, are the most effective in this process;[19] on the other hand, copper's biggest problem is the leaching of Cu ions in water, ETBE and TAME were selected as a model molecule due to the great problem of the presence of gasoline oxygenates in rivers, lakes and groundwater,[20] which is necessary to propose various destruction techniques.

2. Results and Discussion

Figure 1 shows the results of the nitrogen adsorption-desorption process of all materials. In part a, the impregnated samples presented isotherms type IVa with hysteresis type H2 and the volume of nitrogen was increased with the 5% by weight of copper material, however, the materials prepared by sol gel, showed Isotherms type a, and presented two hystereses (b). Regarding the pore diameter distribution, the impregnation samples exhibited a range between 20 and 90 Å, only the sample with 5% copper was bimodal (c). A similar behavior had the samples synthesized by sol gel but with a range between 50 to 300 Å, which is higher than the impregnated samples (d).

As for the surface area, calculated by the BET equation, the sol gel samples are 8 times larger than the samples by impregnation, see Table 1. This event indicates that metal

Table 1. Surface area and activity in the dehydration of isopropanol.

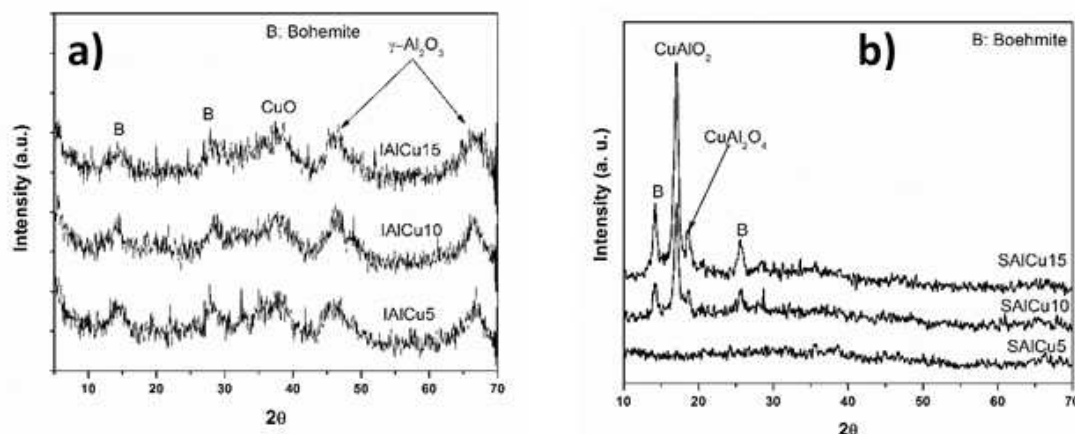| Catalyst	BET Surface area (m^2/g)	Propene selectivity (%)	DIPE selectivity (%)	Rate ($mol\,g^{-1}\,s^{-1}*10^{-6}$)	d (nm)
IAlCu5	26	46	53	5.9	7.1
IAlCu10	43	17	83	1.3	7.3
IAlCu15	30	39.2	60.8	15	7.4
SAlCu5	449	3.2	96.7	16.9	32
SAlCu10	384	49.5	50.4	5.7	35
SAlCu15	370	8.8	91.1	12.4	42

Figure 2. XRD patterns of the catalysts CuO/Al$_2$O$_3$ a) impregnation b) sol gel method.
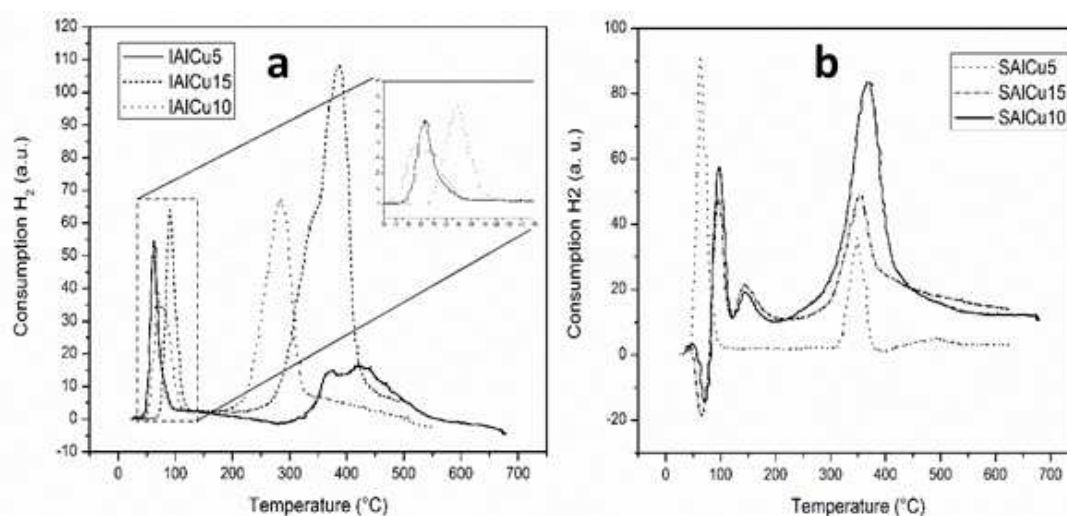

Figure 3. TPR a) Impregnation, b) sol gel method

interactions with active sites of alumina favor high surface areas.[21–24] Figure 2 presents the results of the X-ray diffraction. The structure of the alumina range in the impregnated samples was identified, as well as slight diffraction corresponding to the copper oxide (CuO),[25–31] see Figure 2a. Meanwhile, the samples synthesized by sol-gel exhibited the typical diffraction of the boehmite structure, but not those of the copper oxide, instead, the formation of CuAlO$_2$ was favored (Figure 2b). This crystalline structure has been obtained using the synthesis by ball milled or precipitation, and its subsequent thermal treatment at high-temperature conditions.[32] This structure can also be achieved through the orientation when depositing on a substrate of silica oxide.[33]

The specific synthesis and orientation under relatively mild conditions of this structure through the sol gel method is relevant. Even with this, the formation of copper aluminate spinel (CuAl$_2$O$_4$, 2θ:18.91°) was also favored. This structure, as well as CuAlO$_2$, has been achieved by using high-temperature thermal treatments.[34] Figure 3a shows the reduction profiles of

impregnated materials. The consumption of hydrogen around 100°C corresponds to the CuH formation, while the consumption of hydrogen around 350°C is due to the reduction of Cu^{2+}−Al. interactions. On the other hand, the reduction of surface copper oxide is originated at 400°C.[35] The 10% sample is the only one that shows a Cu−Al^{2+} interaction. In Figure 3b, SAlCu5 sample presented the corresponding reduction to copper oxide around 100°C. The reduction of Cu^{2+}Al was performed at 350°C. The samples SAlCu15 and SAlCu10 displayed a reduction profile different from the sample SAlCu5. A hydrogen consumption was presented at 100 and 150°C. Based on the X-ray diffraction pattern (Figure 2(b)), the compound CuAlO$_2$ showed a greater diffraction intensity with respect to CUAl$_2$O$_4$, therefore; the abundance of CuAlO$_2$ is greater than the one of CuAl$_2$O$_4$. Taking this information into account, the reduction to 100°C corresponds to the compound CuAlO$_2$ and the reduction of CuAl$_2$O$_4$ is favored at 150°C (Figure 3a and 3b).
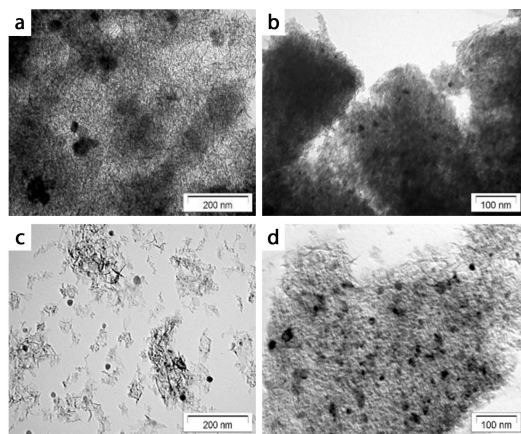
Figure 4. STEM for the catalysts CuO/γ-Al$_2$O$_3$ a) and b) Method of impregnation 10 and 15% c) and d)) Sol gel method 10 and 15%.

The STEM images of the impregnated samples are shown in Figure 4a and 4b. Whereas the TEM images of the sol gel materials are shown in Figure 4c–4d.

Here it is observed that some copper is interacting with alumina to form copper aluminate with remnants of oxide copper particles on the surface using sol gel method, which are larger than 20 nm and has been previously reported at temperatures below 600 °C.[36] This result coincides with the particle size distribution (d) reported in Table 1 and shown in the histogram of Figure 5b.

While for the impregnated samples a unimodal distribution was obtained, in the Figure 5a for to estimate the particle size value for Copper; resulting in an average size of 7 nm in the three samples (Table 1).

In the decomposition of isopropanol, the main product that is obtained is the olefin and the rate of dehydration is directly related to the concentration of total acidity sites of the catalyst.[37–39]

The selectivity for isopropanol dehydration provides important information about the acidity of the catalyst. Propene and di-isopropyl ether (DIPE), are the main products of the reaction. The formation of propene is related to the strength of the acid
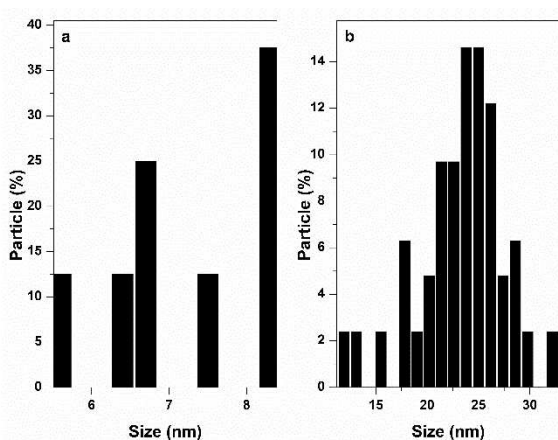
site, whereas the formation of DIPE is almost a consequence of the concentration of acid sites.[28] Table 1 reports activity and selectivity for dehydration of isopropanol.

The SAlCu5 sample showed the best behavior, among the materials prepared by the sol gel method, to describe a higher concentration of acid sites in the solid (DIPE: 96.7% and isopropanol dehydration rate: 16.9 mol g-1 s-1*10-6). However, for materials impregnated according to the isopropanol dehydration rate, the material with the best acidity on the surface is the sample IAlCu15. The increasing order of surface acidity in all the materials analyzed is mentioned below:

IAlCu15 > IAlCu5 > IAlCu10;

SAlCu5 > SAlCu15 > SAlCu10

On the other hand, the surface acidity was higher for samples IAlCu5 (46%) and SAlCu10% (49.5%). Although the impregnated materials exhibited a low concentration of acid sites, compared to those of sol gel, these sites have a higher acid strength.

Previously our research group has reported on the presence of acid sites in alumina, modified with other semiconductors (CeO$_2$) and noble metals (Rh and Sn) as active sites in catalysts, has an important role in the reaction mechanism for Catalytic Wet Air Oxidation (CWAO) of oxygenated organic compounds, as proposed in this work. Since at a higher concentration of acid sites there are fewer intermediates, such as tert-butanol, 2-methylpropene, acetone and methanol, which allows complete mineralization to CO$_2$. The importance of this work lies mainly in obtaining catalytic materials with greater acidity for the complete oxidation of oxygenated compounds without generating reaction intermediates and replace to use of noble metals as active sites which have a high cost.[40–42] The greater presence of acidity in the materials modified with copper by sol gel is possibly due to the interaction between this metal with the alumina to form the copper aluminate spinel which consequently has a significant effect on the catalytic activity.

Table 2 shows the catalytic activity of all samples tested in the CWAO of ETBE and TAME. It is evident that the samples prepared by the sol gel method had a better catalytic behavior, which indicates that the activity of these materials is a function of the number of surface acid sites, the smaller particle size of the Cu and the surface of the contact, in the case of the ETBE, because the SAlCu5 material was the most active. For the

Figure 5. Particle size distribution samples IAlCu15 (a), SAlCu15 (b).

Table 2. Initial rate (r_i) TOC abatement (X_{TOC}%), ETBE and TAME Conversion (X%) and initial rate in CWAO with CuO supported catalysts.

Catalyst	ETBE			TAME		
	X_{TOC} (%)	X (%)	r_i (mmol g^{-1} s^{-1})	X_{TOC} (%)	X (%)	r_i (mmol g^{-1} s^{-1})
IAlCu5	76	76	0.62	72	72	0.52
IAlCu10	66	66	0.27	68	68	0.44
IAlCu15	72	72	0.55	77	77	0.43
SAlCu5	82	82	0.75	73	73	0.34
SAlCu10	88	88	0.55	70	72	0.61
SAlCu15	80	80	0.54	78	78	0.60

TAME, the activity was based mainly on the strength of the present acid sites and the presence of the copper aluminate spinel, which possibly increased the strength of the acid sites, but by increasing the amount of Cu in the materials, the acidity diminishes, for which, we can establish that at 10% of Cu there is the highest surface acidity strength due to the formation of the copper aluminate spinel, as shown by the SAlCu10 material. Among the impregnated materials, the IAlCu5 sample showed the best catalytic activity with the two contaminating molecules (ETBE and TAME), this is mainly attributed to the smaller particle size of the Cu and the greater strength of the surface acid sites in the material. According to the catalytic activity, high sensitivity of the acid sites was observed in the degradation of ETBE, while for TAME it was due to the presence of the species $CuAlO_2$ and $CuAl_2O_4$.

Previously, our research group has reported the catalytic activity of materials prepared with alumina at different contents of Cu (5, 10 and 15%) as an active phase, synthesized by methods such as sol gel, impregnation and impregnation modified with urea, used in the CWAO of ETBE and TAME. The activity of these materials in the CWAO of ETBE, reveals that CO_2 selectivity is complete with all the materials prepared by the impregnation method, with the sol gel method the catalysts are completely selective only up to 10% Cu and with the method of impregnation modified with urea no material was totally selective to CO_2.[43] Comparing the above, with the results obtained in this investigation we observe that in this work all the catalysts prepared have a CO_2 selectivity of 100% in the CWAO of the ETBE, which describes a greater efficiency in the materials. In the case of TAME, the work presented above only describes that the material prepared by the sol gel method with 15% Cu and the material synthesized by impregnation modified with urea with 5% Cu, are the only ones that complete the CO_2 selectivity with this pollutant model molecule. However, in this investigation only the material prepared with the sol gel method at 10% of Cu was the only one that did not complete its CO_2 selectivity, this shows that the materials synthesized in this work show a better catalytic behavior in the CWAO of ETBE and of the TAME.

On the other hand, alumina catalysts with a Cu content of 5%, similar to those shown here, have been used in the CWAO of the phenol at 3 hours of reaction describing its catalytic behavior both in the oxidized state and in the reduced state, where better catalytic behavior occurs in the first case. However, the incorporation of a third element such as 5% Ce in the alumina interacting with the same Cu content improves twice the activity in the phenol CWAO, both in the oxidized and reduced state in the catalyst.[44] This turns out to be as relevant as what happened in the 90's when Striolo et al used three different homogeneous catalysts (Fe—Cu—Mn) in the CWAO of organic acids, which showed that the synergy between the three metals considerably improves the activity in comparison when only two or one catalysts was used in the system.[45] The above described leaves us with important evidence so that soon this type of catalysts can interact as shown here, with other elements or oxides that synergistically can significantly improve the activity in the CWAO.

Table 3. Selectivity to CO_2 and leaching of Cu in CWAO of ETBE and TAME with CuO supported catalysts.

Catalyst	ETBE		TAME	
	S_{CO_2}(%)	Cu leaching (ppm)	S_{CO_2}(%)	Cu leaching (ppm)
IAlCu5	100	0.272	100	0.011
IAlCu10	100	0.306	100	0.020
IAlCu15	100	0.531	100	0.032
SAlCu5	100	0	100	0
SAlCu10	100	0	97	0
SAlCu15	100	0	100	0

Table 3 shows the selectivity to CO_2 formation at the end of the reaction of ETBE and TAME. In the case of ETBE, all the materials showed 100% of the selectivity to CO_2, which can be explained by the acid sites quantity and related by the DIPE formation selectivity showed in Table 1. In the case of TAME, only the sample SAlCu10 showed incomplete selectivity to CO_2 but the value was high too (97%). It is important to note that this sample was the one that showed the lowest selectivity value to the DIPE, which shows that this reaction is more sensitive to the presence of acid sites in the catalyst than in ETBE case. This may be due to the fact that the molecular structure of TAME contains a methyl group more compared to ETBE, which possibly forms intermediates of alkenes, ketones and alcohols with a higher aliphatic chain, which require greater acidity to later transform to CO_2 and H_2O.

Table 3 shows the results of the process of leaching of Cu in the materials evaluated in the CWAO of ETBE and TAME. Here we can observe that the materials synthesized by the sol gel method do not present this phenomenon. These can be attributed to the formation of copper spinel ($CuAlO_2$ and $CuAl_2O_4$) due to the sol-gel preparation method and observed in the analysis of X-ray diffraction (Figure 2b) and TPR (Figure 3b) analysis. Contrary, in the case of the catalysts synthesized by the impregnation method, the leaching of Cu ions with the amount of 0.531 ppm using IACu15 catalyst in the CWAO of ETBE which represents 3.54% of the copper in the reaction milieu.

The materials shown in this study have better stability and resistance to leaching, a series of catalysts similar to ours have been reported in both composition and synthesis, varying only the calcination temperature in the final thermal treatment and reaction conditions (mild conditions for two hours) in the phenol CWAO (see Table 4). From here it was observed that at elevated temperatures the leaching is considerably reduced by the presence of active species of Cu on the surface of the material, but as the treatment temperature decreases from 650 to 450 °C in the catalysts the amount of leached Cu increases in the system,[46] this reveals that the materials analyzed, evaluated and heat-treated at 400 °C have a greater stability of the active phase even after subjecting them to pressure and temperature conditions, where the materials prepared by sol gel do not show amount of leached Cu. The Table 4 summarizes the catalytic behavior, reaction conditions and leaching of Cu in materials like solids analyzed in this work. In most of the materials compared in Table 4 they show copper leaching in

Table 4. Bibliographic description of the catalytic behavior of materials with Cu applied in the CWAO at different conditions.

Catalyst (%Cu) – preparation method	Pollutant Model Molecule	Reaction Conditions	Activity (rate, % conversion or % oxidation)	Cu leaching (% or ppm)	Reference
Cu (5, 10, 15%)/Al$_2$O$_3$ – impregnation and sol gel	ETBE/TAME	100 °C, 10 bar, 1 hour, 1000 ppm of pollutant	TOC > 74%	N.M	[43]
Cu (5%)/Al$_2$O$_3$, Cu (5%)/ Al$_2$O$_3$–CeO$_2$ – impregnation	Phenol	120 °C, 10 bar, 3 hours, 1000 ppm of pollutant	Rate: 341 and 809 mmol/ hg$_{phenol}$	N.M	[44]
Fe, Cu, Mn (Homogeneous)	Mixture of organic acids	98 °C, H$_2$O$_2$, pH 3,5	TOC > 90%	N.M	[45]
Cu (5%)/Al$_2$O$_3$ – impregnation (400, 650 and 900 °C)	Phenol	40 and 70 °C, 1 atm, 2 hours, H$_2$O$_2$,1000 ppm of pollutant	TOC > 86%	36-64%	[46]
Cu (10%)/Al$_2$O$_3$ – impregnation (550 °C)	Phenol	140 °C, 0.5 Mpa, 5 hour, pH 6, 0.047 mol/L of pollutant	Rate: 0.4 L/hg$_{cu}$ to pH 7	58%-1% depending on the pH	[47]
Cu/Al$_2$O$_3$–Cu/Al$_2$O$_3$–CeO$_2$ impregnation (450 °C)	Methylene blue	180 °C, 1.5 Mpa, 2 hours, 2000 ppm of pollutant	COD:74.5% for Cu/Al$_2$O$_3$ and 84.6% for Cu/Al$_2$O$_3$–CeO$_2$	28.2 ppm for Cu/Al$_2$O$_3$ and 2.9 ppm for Cu/Al$_2$O$_3$–CeO$_2$	[48]
Cu–Fe/Al$_2$O$_3$–Cu–Fe–La/ Al$_2$O$_3$ impregnation (450 °C)	Methyl orange	200 °C, 2 Mpa, 2 hours, 4000 ppm of pollutant	COD:84.5% for Cu–Fe/Al$_2$O$_3$ and 91.4% for Fe–La/Al$_2$O$_3$	7.5 ppm for Cu–Fe/Al$_2$O$_3$ and 3.8 ppm for Cu–Fe–La/Al$_2$O$_3$	[49]

NM: Not measured.

different quantities, which in some cases depends on the pH, the addition of an element or the treatment temperature. In our materials we observe that using the method of sol gel preparation this phenomenon does not occur, which is beneficial for the reaction conditions used here, these materials show good resistance and activity in the CWAO of ETBE and TAME, and offer the possibility to be reused and economically manufactured for the low cost of Cu compared to metal elements such as Au, Ag, Pt, Pd, Ru and Rh.

3. Conclusions

The incorporation of copper in alumina facilitated the modification of textural properties. By impregnation, only the presence of the CuO and boehmite phase of the alumina was identified, while the species CuAlO$_2$ and CuAl$_2$O$_4$ by sol gel were observed. In the impregnation materials, the Cu–Al^{2+} interaction is favoured, which possibly inhibits the activity and concentration of acid sites of the catalyst with 10% copper for these materials. The catalytic activity is attributed to the smaller particle size of the Cu and the greater strength of the surface acid sites for both polluting molecules using IAlCu5 as a catalyst. Nevertheless, the materials prepared by sol gel they act differently depending on the contaminating molecule. SAlCu5 was the most active in the ETBE oxidation due to the number of surface acid sites, the smaller particle size of the Cu and the surface of the contact. Meanwhile, SAlCu10 showed the most activity in the CWAO of TAME by the strength of the present acid sites and the presence of the copper aluminate spinel and the CuAlO$_2$ which manifest greater interaction Cu–Al.

The CWAO of TAME reaction is more sensitive to the presence of acid sites in the catalyst than ETBE. The materials presented in this study would possibly have a similar catalytic behavior if compared with other modified catalysts and added with active sites of noble metals, which would present an advantage due to the low cost of copper. Formation of the spinel species in the copper catalysts prepared by sol-gel

method inhibits leaching of the copper ions in the reaction milieu, which it's an advantage in comparison with the classical method of preparation by impregnation.

Experimental Section

Catalyst Preparation

The first series of materials were loaded with Cu by the impregnation method to obtain 5%, 10% and 15% by weight. For which, boehmite (Boehmite Catapal B) was placed in a solution with a pH of 3 by nitric acid (HNO$_3$, Baker at 66%); the temperature was increased to 70 °C. Subsequently, copper nitrate (Cu(NO$_3$)$_2$ 1/2 H$_2$O Baker 99%) was added to the solution until the mixture was homogenized. The temperature was raised to 90 °C for 4 hours. The solvent was removed under vacuum and dried at 120 °C. The resulting materials were calcined at 400 °C for 4 hours. The following series of materials was prepared by the sol gel method from the hydrolysis of titanium trisecbutoxide (Sigma Aldrich 97%) mixed with deionized water, secbutanol (Sigma Aldrich 99.5%), urea (JT Baker, 99%) and copper nitrate hydrate (Baker 99%) to form a sol that was left in aging at reflux conditions at 70 °C for 24 hours. Then the solid was separated from the solvents using a rotary evaporator in vacuum at 60 °C, which was dried at 120 °C for 24 hours until a powder was obtained which was calcined at 400 °C for 4 hours.

For identification, the catalysts impregnation (I), sol-gel (S), alumina (Al) and cupper (Cu) were labelled as IAlCuX a SAlCuX, where X (5 10 and 15 wt% of copper).

Characterization Techniques

BET Specific Surface Area

The BET specific surface area was carried out in an automatic Quantachrome Autosorb 3B analyzer. The Nitrogen adsorption isotherms were conducted at −196 °C;the samples were outgassed overnight at 300 °C prior to the nitrogen adsorption. The specific surface area was calculated from the adsorption isotherms by the BET method.

X-Ray Diffraction (XRD)

The crystalline phase composition of the obtained materials was determined on a Siemens D-500 instrument using Cu−Kα radiation ($\lambda = 1.5418$ Å). The reflection intensities were measured by step scanning in the 2θ range between 10–70° with a step size of 0.02° and a scan speed of 4° min^{-1}.

Temperature Programmed Reduction under H$_2$ Atmosphere (H2-TPR)

H$_2$-TPR experiments were performed in a CHEMBET-3000 (QUAN-TACHROME Co) equipment using 0.2 g of the catalyst by means of the following protocol: samples were heated at 300°C under nitrogen flow (10 mL min^{-1}) during 30 min. Then, the samples were cooled down to room temperature and mixed gas flow (5% H2/95% N$_2$) was passed through the cell. The TPR profiles were registered using a heating program of 10°C min^{-1} from room temperature up to 700°C using a flow rate of the gas mixture of 10 mL min^{-1}.

Transmission Electron Microscopy (TEM)

STEM images were obtained on a Tecnai G2 F30 instrument. The sizes of Cu/Al$_2$O$_3$ nanoparticles were obtained by measuring 200 particles for each sample.

Isopropanol Dehydration

The isopropanol dehydration was carried out at atmospheric pressure and 130°C over pre-activated catalysts (400°C 2 h, in fluxed nitrogen). The isopropanol was fed by using a saturator system coupled to a fixed bed glass reactor (with a volume of 3 ml and using 20 mg of catalyst). The HGSV used for the isopropanol dehydration was 1 h^{-1}. The activity was followed by determining the isopropanol conversion and the selectivity was determined for propene and di-isopropyl ether (DIPE). The analysis of products was carried out with a gas chromatograph VARIAN CP-3800 coupled to the catalytic activity system and equipped with a capillary Quadrex Stationary phase, 007-FFAP with 30 m of length.

Reaction Conditions

The catalytic wet air oxidation reaction was carried out in a batch reactor of stainless steel high-pressure (Parr Instruments) coated with a glass liner to prevent corrosion problems. The volume of reaction was 150 mL of an aqueous contaminant (ETBE, TAME) solution with a concentration of 1000 ppm and 1 g/L^{-1} of catalyst, then nitrogen was introduced into the reactor during 15 min to remove the air contained and after this the reactor was heated at 100°C. Afterwards, an oxygen (high purity) pressure of 10 bar was introduced into the reactor and under continuous agitation of 1000 rpm, the reaction was initiated. Previous test reactions showed that under such conditions the reaction rate was not controlled by the diffusion of oxygen into the liquid phase. The evolution of the reaction was followed by performing the analysis of aliquots at intervals of 10 min through 1 h. The aliquots were taken from the reactor using the sampler valve equipped with a microspore glass filter to prevent the catalyst loss and analyzed on a gas chromatograph (Varian 3400Cx) equipped with a flame ionization detector (FID) on a capillary column HP-into wax. The initial rate (ri) was calculated from the pollutant (ETBE or TAME) conversion as a function of time curves, using the following equations:

$$r_i = (\Delta Conv(\%)/\Delta t)(60[pollutant]_i)/m_{cat} \qquad (1)$$

The analysis of total organic carbon (TOC) was performed by using a 5000 TOC Shimadzu Analyzer, which was previously calibrated to obtain concentrations in the range of 0–1000 ppm of TOC (Eq. (2)); TOC^f = after 1 h of reaction and TOC^i at t = 0.

$$X_{TOC} = \left(\left([TOC]^i - [TOC]^f\right)/[TOC]^i\right)*100 \qquad (2)$$

The selectivity to CO$_2$ was calculated using the following equation:[50]

$$S_{CO_2} = \frac{\Delta TOC}{X_{(pollutant)}} x\ 100\% \qquad (3)$$

Leaching of Cu in the Employed Catalysts in CWAO of ETBE and TAME

Atomic absorption analysis of the samples after the reaction was carried out using a Perkin Elmer apparatus equipped with a graphite fur using a lamp of copper ions to determinate the concentration of this ion in the reaction milieu in order to study the leaching phenomenon in the CWAO of ETBE and TAME. The calibration curves were makes before analysis in the range of the 0 to 20 ppm of copper.

Conflict of Interest

The authors declare no conflict of interest.

[1] P. W. Selwood, *Adv. Catal.* **1951**, *3*, 27–106.
[2] S. J. Tauster, S. C. Fung, R. L. Garten, *J. Am. Chem. Soc.* **1978**, *100*, 170–175.
[3] I. E. Wachs, *Catal. Today* **1996**, *27 (3–4)*, 437–455.
[4] B. M. Reddy, P. M. Sreekanth, Y. Yamada, Q. Xu, T. Kobayashi, *Appl. Catal. A* **2002**, *228*, 269–278.
[5] S. A. Hassanzadeh-Tabrizi, R. Pournajaf, A. Moradi-Faradonbeh, S. Sadeghinejad, *Ceram. Int.* **2016**, *42*, 14121–14125.
[6] G. J. Hutchings, A. A. Mirzaei, R. W. Joyner, M. R. H. Siddiqui, S. H. Taylor, *Appl. Catal. A* **1998**, *166*, 143–152.
[7] I. P. Chen, S. S. Lin, C. H. Wang, L. Chang, J. S. Chang, *Appl. Catal. B* **2004**, *50*, 49–58.
[8] C. G. Aguilar, C. E. Moreno, *J. Mater. Sci.* **2018**, *53*, 1646–1657.
[9] N. Yang, H. Sun, *Coord. Chem. Rev.* **2007**, *251*, 2354–2366.
[10] A. Nosal-Wiercińska, *J. Electroanal. Chem.* **2011**, *654*, 66–71.

[11] N. E. Rajeevan, R. Kumar, D. K. Shukla, P. P. Pradyumnan, S. K. Arora, I. V. Shvets, *Mater. Sci. Eng. B* **2009**, *163*, 48–56.

[12] J. A. Zazo, J. A. Casas, A. F. Mohedano, J. J. Rodríguez, *Appl. Catal. B* **2006**, *65*, 261–268.

[13] Y. Tang, K. Shih, K. Chan, *Chemosphere* **2010**, *80*, 375–380.

[14] L. Oliviero, J. Barbier, D. Duprez, A. Guerrero-Ruiz, B. Bachiller-Baeza, I. Rodriguez-Ramos, *Appl. Catal. B* **2000**, *25*, 267–275.

[15] A. Quintanilla, J. A. Casas, A. F. Mohedano, J. J. Rodríguez, *Appl. Catal. B* **2006**, *67*, 206–216.

[16] A. Pintar, M. Besson, P. Gallezot, *Appl. Catal. B* **2001**, *31*, 275–290.

[17] L. Oliviero, J. Barbier, D. Duprez, H. Wahyu, J. W. Ponton, I. S. Metcalfe, D. Mantzavinos, *Appl. Catal. B* **2001**, *35*, 1–12.

[18] L. Oliviero, J. Barbier, D. Duprez, *Appl. Catal. B* **2003**, *40*, 163–184.

[19] Z. Lockman, L. P. Lin, C. K. Yew, S. D. Hutagalung, *Sol. Energy Mater. Sol. Cells* **2009**, *93,* 1383–1387.

[20] A. N. Banerjee, R. Maity, P. K. Ghosh, K. K. Chattopadhyay, *Thin Solid Films* **2005**, *474*, 261–266.

[21] K. A. Cychosz, R. Guillet-Nicolas, J. García-Martínez, M. Thommes, *Chem. Soc. Rev.* **2017**, *46*, 389–414.

[22] Q. J. Liu, Z. T. Liu, *Vacuum* **2014**, *107*, 90–98.

[23] Y. Lu, T. Nozue, N. Feng, K. Sagara, H. Yoshida, Y. Jin, *J. Alloys Compd.* **2015**, *650*, 558–563.

[24] A. N. Banerjee, C. K. Ghosh, K. K. Chattopadhyay, *Sol. Energy Mater. Sol. Cells* **2005**, *89*, 75–83.

[25] M. Fang, H. He, B. Lu, W. Zhang, B. Zhao, Z. Ye, J. Huang, *Appl. Surf. Sci.* **2011**, *257*, 8330–8333.

[26] N. Wolff, D. Klimm, D. Siche, *J. Solid State Chem.* **2018**, *258*, 495–500.

[27] I. Hamada, H. Katayama-Yoshida, *Phys. B* **2006**, *376–377*, 808–811.

[28] T. Suriwong, T. Thongtem, S. Thongtem, *Curr. Appl. Phys.* **2014**, *14*, 1257–1262.

[29] C. L. Jiang, Q. J. Liu, F. S. Liu, Z. T. Liu, *Curr. Appl. Phys.* **2017**, *17*, 126–129.

[30] K. Vojisavljević, B. Malič, M. Senna, S. Drnovšek, M. Kosec, *J. Eur. Ceram. Soc.* **2013**, *33,* 3231–3241.

[31] C. Ruttanapun, W. Kosalwat, C. Rudradawong, P. Jindajitawat, P. Buranasiri, D. Naenkieng, N. Boonyopakorn, A. Harnwunggmoung, W. Thowladda, W. Neeyakorn, C. Thanachayanont, A. Charoenphakdee, A. Wichainchai, *Energy Procedia* **2014**, *56*, 65–71.

[32] M. Senna, P. Billik, A. Y. Yermakov, M. Škrátek, M. Majerová, M. Čaplovičová, M. Mičušík, L. Čaplovič, M. Bujdoš, M. Nosko, *J. Alloys Compd.* **2017**, *695,* 2314–2323.

[33] K. Kamiya, T. Yoko, Y. Miyaji, K. Matusita, *Int. J. High Technol. Ceram.* **1987**, *3*, 297–307.

[34] R. H. Jarman, J. Bafia, T. Gebreslasse, B. J. Ingram, J. D. Carter, *Mater. Res. Bull.* **2013**, *48*, 3916–3918.

[35] R. N. Pease, H. S. Taylor, *J. Am. Chem. Soc.* **1921**, *43*, 2179–2188.

[36] S. N. Alam, N. Sharma, D. Panda, A. Kumar, D. Sampenga, A. Sairam, V. Sarky, M. B. Krupateja, *J. Alloys Compd.* **2018**, *753*, 799–812.

[37] C. Bouzidi, H. Bouzouita, A. Timoumi, B. Rezig, *Mater. Sci. Eng. B* **2005**, *118*, 259–263.

[38] C. H. Ong, H. Gong, *Thin Solid Films* **2003**, *445*, 299–303.

[39] M. Miclau, N. Miclau, R. Banica, D. Ursu, *Mater. Today* **2017**, *4*, 6975–6981.

[40] I. Cuauhtemoc, G. Del Angel, G. Torres, V. Bertin, *Catal. Today* **2008**, *133–135*, 588–593.

[41] A. Cervantes, G. Del Angel, G. Torres, G. Lafaye, J. Barbier Jr., J. N. Beltramini, J. G. Cabanas-Moreno, A. E. de los Monteros, *Catal. Today* **2012**, *212*, 2–9.

[42] I. Cuauhtémoc, G. Del Angel, G. Torres, C. Angeles-Chavez, J. Navarrete, J. M. Padilla, *Catal. Today* **2011**, *166*, 180–187.

[43] Z. Guerra Que, J. G. Torres Torres, I.Cuauhtemoc Lopez, J. C. Arevalo Perez, A. Cervantes Uribe, H. Perez Vidal, A. E. de los Monteros Reyna, J. G. Pacheco Sosa, M. A. Lunagomez Rocha, C. Sanchez Trinidad, "Nonconventional Wastewater Treatment for the Degradation of Fuel Oxygenated (MTBE, ETBE, and TAME)" **2019**, 10.5772/intechopen.84250, pp. 1–20.

[44] Z. Guerra-Que, H. Perez-Vidal, G. Torres-Torres, J. C. Arevalo-Perez, A. A. Silahua-Pavon, A. Cervantes-Uribe, A. E. de los Monteros, M. A. Lunagomez-Rocha, *RSC Adv.* **2019**, *9*, 8463–8479.

[45] P. Striolo, J. N. Foussard, H. Debellefontaine, Proceedings of the 1st International Conference on Advanced Oxidation Technologies for Water and Air Remediation, London, Ontario, Canada, June 25–30, **1994**, pp. 363–365.

[46] A. Devard, P. Brussino, F. A. Marchesini, M. A. Ulla, *J. Environ. Chem. Eng.* **2019**, *7*, 103201.

[47] R. R. Sapico, P. Marin, F. V. Diez, S. Ordoñez, *J. Environ. Chem. Eng.* **2017**, *5*, 2570–2578.

[48] Y. Zhang, Y. Zhou, C. Peng, J. Shi, Q. Wang, L. He, L. Shi, *Appl. Surf. Sci.* **2018**, *436*, 981–988.

[49] Y. Zhang, F. Peng, Y. Zhou, *Chin. J. Chem. Eng.* **2016**, *24*, 1171–1177.

[50] S. S. Lin, D. J. Chang, C.-H. Wang, C. C. Chen, *Water Res.* **2003**, *37*, 793–800.